Structures 27 (2020) 343–351

Contents lists available at ScienceDirect

Structures

journal homepage: www.elsevier.com/locate/structures

Corroded RC beam repaired in flexure using NSM CFRP rod and an external steel plate

Belal Almassri[a,*], Abdulsamee M. Halahla[b]

[a] Civil and Arch. Engineering Department, College of Engineering, Palestine Polytechnic University, Hebron, Palestine
[b] Department of Civil Engineering, College of Engineering, Fahad Bin Sultan University, Tabuk, Saudi Arabia

A R T I C L E I N F O

Keywords:
RC beams
Steel corrosion
NSM CFRP
External steel plates
Repair
FEM
CDP

A B S T R A C T

Repairing Corroded Reinforced Concrete (RC) beams has been an important area of study so far. Restoring the mechanical properties of (RC) beams which have been lost due to steel corrosion is necessary to maintain the required service life and load capacity of any (RC) structure. Despite the noticeable increase which was found during the experimental test in terms of moment capacity, stiffness and ductility of a repaired beam, the repaired corroded beam failed as a result of a premature mode of failure by the separation of concrete cover. In this paper, an analytical and Finite Element (FE) investigation are conducted on a corroded RC beam which was previously repaired with near surface mounted technique (NSM) using carbon fibre polymer rods (CFRP). A (FE) model using the commercial program ABAQUS was produced to predict the moment-deflection behavior and crack/failure pattern, it was found that using an external steel plate increases the ultimate capacity and stiffness, and it changes the mode of failure of the repaired corroded beam from a non-conventional failure mode, in which the beam cover exfoliates, to a classical and more ductile one by causing tensile reinforcement to yield, and concrete to subsequently crush in the compressed region.

1. Introduction

Methods of high reliability are increasingly needed to measure the ultimate capacity and the service life left for deteriorated reinforced concrete (RC) structures as an important requirement for different repair strategies [1,2]. Corrosion of steel reinforcement represents the major reason behind the deterioration of (RC) structures. The corrosion process entails serious structural damages: longitudinal cracks in concrete cover due to expansive corrosion products; loss of cross-sectional area of steel bars; the bond deterioration between concrete and steel reinforcement bars, and a serious decrease in the ultimate strain of reinforcing bars "reduction in steel bars ductility" [3–6]. Consequently, a considerable reduction occurs in the service life and the ultimate capacity of (RC) elements.

To restore the service life and the load capacity of reinforced concrete structures which have been lost due to steel corrosion, it is required to repair them using suitable available engineering techniques. Several experimental and numerical modelling studies presented the flexural and shear response of RC elements strengthened using epoxy bonded steel plates [7–10], Arslan et al. [11] showed that the external steel plate was highly effective on improving the flexural behavior of previously damaged slender RC beams. Recently, there have been several studies on the (RC) elements strengthened with externally bonded fibre-reinforced polymer EBR (FRP) laminates [12–14]. Another strength-enhancing technique called Near Surface Mounted (NSM) which uses also the composite material FRP reinforcement has been employed in the research and practical engineering solutions [15–17]. In this technique, concrete cover has to be grooved, through which FRP reinforcement is bonded. This is followed by filling the grooves with epoxy or cement grout.

Kreit et al. [18] and Almassri et al. [19] investigated the possibility of flexural repairing naturally corroded RC beams using NSM CFRP rods. It was found that the NSM technique increased the load bearing capacity of the corroded beam to a high degree. The corroded beams with significant reduction in steel bars cross-sectional area exhibited an ultimate capacity similar to the control "Non-corroded" beam. The NSM CFRP technique slightly raised the stiffness of the repaired beams and it restored sufficient ductility which had been lost due to steel reinforcement corrosion.

The FE numerical modelling was used several times in the literature to construct models which can predict the overall behavior of concrete elements subjected to NSM strengthening. Hawileh [20] used the experimental results conducted by Almahmoud et al. [21], and constructed a model using ANSYS software to simulate 4-point loaded RC

* Corresponding author.
E-mail address: mbelal@ppu.edu (B. Almassri).

https://doi.org/10.1016/j.istruc.2020.05.054
Received 21 November 2019; Received in revised form 21 May 2020; Accepted 26 May 2020

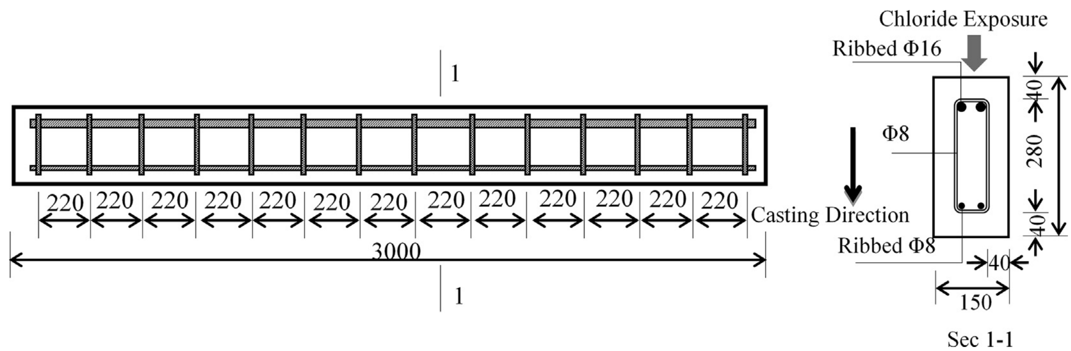

Fig. 1. Reinforcement layout of type A beams. (Dimensions are all in mm).

beams for predicting their ultimate capacity. Barros et al. [22] used the computed code FEMIX to construct a multi-directional smeared cracking model for compression and tension behavior of RC beams shear repaired with NSM CFRP strips. Almassri et al. [23] used both ABAQUS and FEMIX to predict the behavior of corroded RC beams repaired with NSM in flexure and other non-repaired RC beams. Al-Osta et al. [24] investigated the damage of corroded RC beams by using finite element analysis with different corroded bars and concrete interface models.

Despite the significant advantages of employing NSM in repairing/strengthening of RC beams in flexure, several debonding failure modes have been recorded experimentally, including end debonding failure and intermediate crack induced debonding failure. End cover separation, "Peeling off" as one of the end debonding failure modes, has been found to be by far the most common failure mode [16,17,25,26]

Other corroded RC beams failed by the separation of concrete cover without any detachment of the NSM CFRP rod, this was recorded twice in the tested beams [18,19], The longitudinal pre-loading cracks induced by steel corrosion along concrete cover are the main reason behind this premature mode of failure which limited the efficiency of NSM technique in repairing corroded RC beams [19]. Kreit et al. [27] found the NSM technique efficient in repairing corroded RC beams but it highly depends on the status of the concrete cover deteriorated by steel corrosion.

From the literature it is found that there is an increasing need to prevent non-classical and premature modes of failure such as the separation of concrete cover, Rezazadeh et al. [28] proposed an analytical model to predict the behavior of RC beams strengthened with NSM failed by the separation of concrete cover, it was found that by increasing the length of the NSM FRP in the beam, its failure capacity increases. In another study, Teng et al. [29] suggested a model for NSM (CFRP) strips using a FE study. Furthermore, there has been no research achieved on a large scale which can predict the naturally corroded RC beams behavior as well as simulate the corrosion of steel reinforcement bars through FE numerical modelling. There has not been much research done on this premature mode of failure on NSM-corroded RC beams, due to its complexity as well as the large number of acting parameters involved in this failure. In addition, there have been no studies found to tackle the limitations that face the NSM as a repair technique. After studying all the above-mentioned research gaps and problems, this paper comes to present a FE model using a hybrid strengthening technique; using composite material CFRP rods and also an external steel plate at the same time which can prevent the premature mode of failure by the separation of concrete cover. A 3-D FE model A1CL3-RS is proposed using the commercial software ABAQUS [30], and the model is validated using experimental results from previous published work. This beam is repaired with both NSM CFRP rod in bending as well as an external steel plate at the tension side. The moment-deflection curves, modes of failure, ductility index and stiffness of the repaired corroded RC beams are studied. The current research pays a special attention to the failure modes of the RC beams repaired with NSM only and the one proposed in this paper which is repaired with NSM and external steel plate. It proves that using this hybrid technique would change the failure mode, and it also compares the experimental failure modes to the crack patterns obtained by the FE model.

2. Research significance

In the last years, there has been an increasing need in the engineering society to conserve and rehabilitate the old buildings including the monumental heritage and other important structures like corroded beams and girders in bridges around the world which seized the attention of the researchers. This paper discusses the possibility of using hybrid repair technique for these deteriorated structural elements and opens the door for further investigations in this area.

3. Summary of experimental test

The beam studied in this paper is one of 72 RC beams that were cast in 1984 at LMDC (Laboratory of Materials and Durability of Constructions). The aim of that program was studying the effect of the natural corrosion on the mechanical properties of RC beams. This paper introduces a study on four beams of the same type (type A) with the same geometry shown in Fig. 1. Half of them were exposed to harsh chloride environment and the other half was kept aside to be tested as control beams. More information about this natural corrosion environment can be found in a previous paper [19].

The beams have been subjected to several experimental studies to evaluate cracking resulted from natural corrosion, to quantify chloride content, and to analyze the variation in the mechanical behavior [31,32]. The four RC beams addressed in this work belong to one type (type A) and have identical geometry and reinforcement configuration. However, they are subjected to different values of service loads. More information about the loading and material properties values can be found in [19]. The beams chosen for this study are: A1T-R, A1CL3-R, A2T and A2CL3. Further description and information about their concrete properties is shown in Table 1.

The beams A2CL3 and A2T are non-repaired beams which were tested experimentally to assess the steel corrosion effect. On the other hand, the beams A1CL3-R and A1T-R are repaired by the NSM technique using 6 mm diameter CFRP rod which is installed in the tension side of these beams. The aim is to study the benefits of using the NSM technique to repair naturally corroded RC beams. More information on the detailed procedure of this technique can be found in [18,19]. All beams were subjected to 3-point loading until failure occurred. Fig. 2 displays the experimental moment vs. deflection curves for all RC beams. The experimental results of (A2CL3, A2T, A1T-R and A1CL3-R) are used to verify the FE model.

Table 1
Mechanical characteristics of the concrete at 27 years (average values of 3 tests).

Mechanical characteristics	A1CL3-R	A1T-R	A2T	A2CL3
Beam Description	Corroded repaired beam with NSM CFRP rod	Non-Corroded repaired beam with NSM CFRP rod	Non-Corroded and Non-repaired.	Corroded and Non-repaired
Compression strength (MPa)	62.2	58.9	58.5	61.5
Tensile strength (MPa)	6.85	6	6	6.2
Elastic modulus (MPa)	34 000	30 000	32 000	32 000
Tested Experimentally by	Almassri et al. [19]	Almassri et al. [19]	Dang & Francois [33]	Khan et al. [34]

4. FE numerical model

In the present study, the nonlinear finite element (F.E) is used through ABAQUS to build a 3-D model for a corroded RC beam which was previously repaired using the near surface mounted technique (NSM) with carbon fibre polymer rods (CFRP), and external steel plate, (A1CL3-RS). This innovative hybrid repair system is proposed in order to prevent the brittle failure in the form of separation of concrete cover and to reach the maximum efficiency of NSM. The verification of the FE model is first implemented on the beams which were tested experimentally (A2CL3, A2T, A1T-R and A1CL3-R), then the external steel plate is added to the FE model in order to simulate the global behavior of beam A1CL3-RS.

4.1. Materials properties

In this model, the concrete and the steel plate are simulated using a deformable solid structural element. The steel bars as well as the CFRP rod are represented in the FE model with deformable beam elements, whereas steel stirrups are modeled using truss elements. The epoxy resin material is neglected in this model because by referring to the previous study of Sena Cruz et al. [35], it showed that the influence of the epoxy adhesion on the global behavior and the crack pattern is very low and can be neglected.

4.1.1. Concrete properties

Mainly, there are two material modeling approaches for concrete in ABAQUS, which are the concrete smeared cracking and the concrete damaged plasticity model (CDPM) [36]. Interchangeable use of both models is valid in the case of plain concrete as well as reinforced concrete. In the present study, concrete damage plasticity model is adopted for modelling the concrete. The mechanical properties of concrete are shown in Table 2.

Table 2
Properties of Hardened Concrete Specimens.

Item	$f_c^{'}$(MPa)	ft(MPa)	E_c(MPa)	υ
Value	62.2	6.85	34,000	0.2

Table 3
Parameters of the damage-plasticity model.

Parameter	Value
Dilation angle (ψ)	36°
Eccentricity (e)	0.1
f_{b0}/f_{c0}(ratio of initial equibiaxial compressive yield stress to initial uniaxial compressive yield stress	1.16
K (the ratio of the second stress invariant on the tensile meridian)	0.667
μ (viscosity parameter)	0.0005

Modeling of concrete requires considering a set of parameters according to the CDP model to be able to capture the behavior of concrete accurately. These parameters are summarized in Table 3. These parameters were used by many researchers and the results they obtained had a good agreement with the experimental tests for different structural elements [37–39]. The compression damage parameter (dc) in the CDP model represents the decay in the elastic stiffness due to compressing the concrete, while the tension damage parameter dt represents the decay in the elastic stiffness due to tensioning the concrete. Both parameters are calculated following the method proposed by Lima et al. [40].

The concrete used to build the current FE models is given a compressive strength of 62 MPa and an elasticity modulus of 34,000 MPa. However, Fig. 3 presents the data needed in defining the concrete material in ABAQUS. Fig. 3(a) shows a curve of uniaxial compression

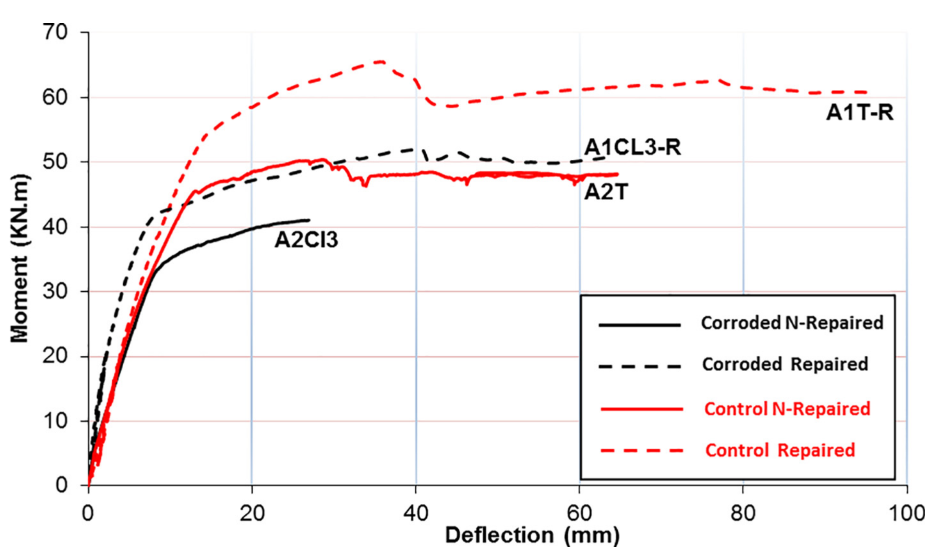

Fig. 2. Experimental Moment-Deflection curves for all beams.

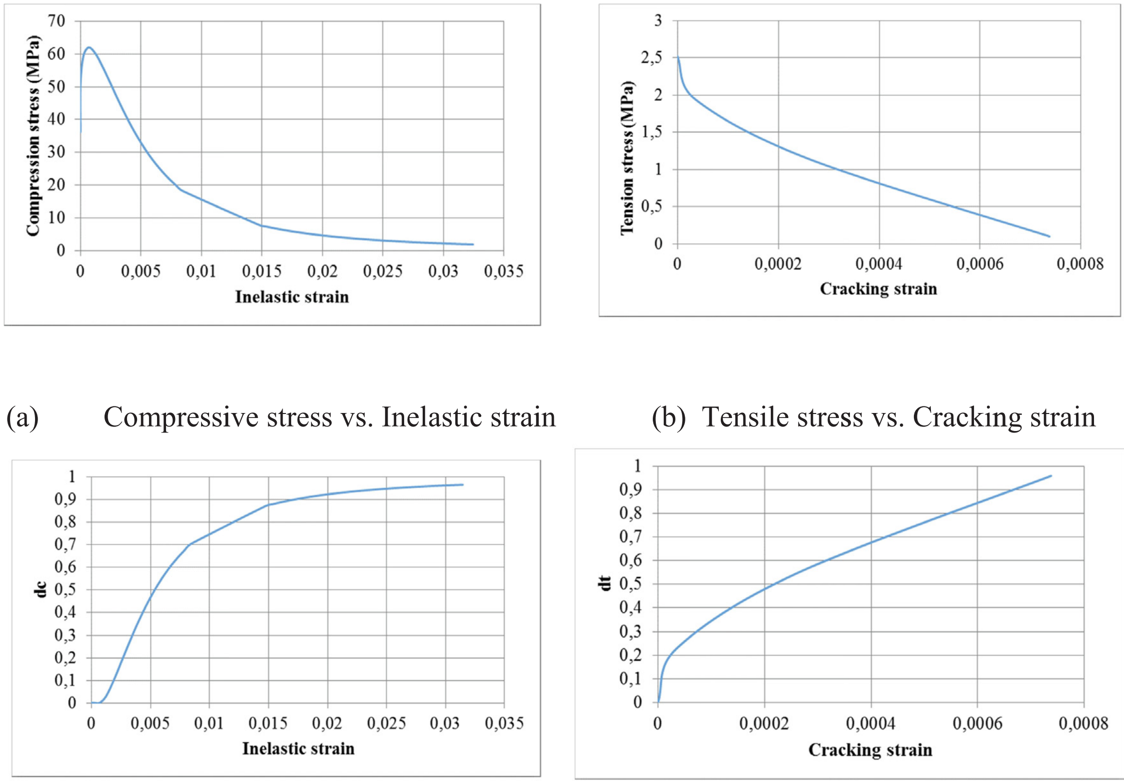

(a) Compressive stress vs. Inelastic strain (b) Tensile stress vs. Cracking strain

(c) Compressive damage vs. Inelastic strain (d) Tensile damage vs. Cracking strain strain

Fig. 3. Definition of concrete parameters for damage-plasticity model.

stress versus inelastic strain of concrete, while Fig. 3(b) shows a curve of tension stress versus cracking strain of concrete, more details of concrete model can be found elsewhere [41,42]. The curve in Fig. 3(c) displays the relation between the compression damage parameter and the inelastic strains, while Fig. 3(d) shows the change in the tension damage parameter at various cracking strains.

4.1.2. Steel bars, steel stirrups and CFRP constitutive models

The behavior of the non-corroded steel reinforcing bars and steel stirrups is assumed elasto-plastic. Fig. 4. Depicts the behavior of the non-corroded steel bars at the post yielding hardening. As reported in the manufacturer's criteria, the CFRP rod keeps having elastic linear stress–strain behavior until it experiences a brittle failure caused by tension (the tensile stress–strain curve for the CFRP provided by both the manufacturer and the laboratory are shown in Fig. 5).

The ordinary ribbed reinforcing steel bars are composed of natural S500 half-hard steels. Some measurements were carried out to determine the properties of the steel bars after the corroded and non-

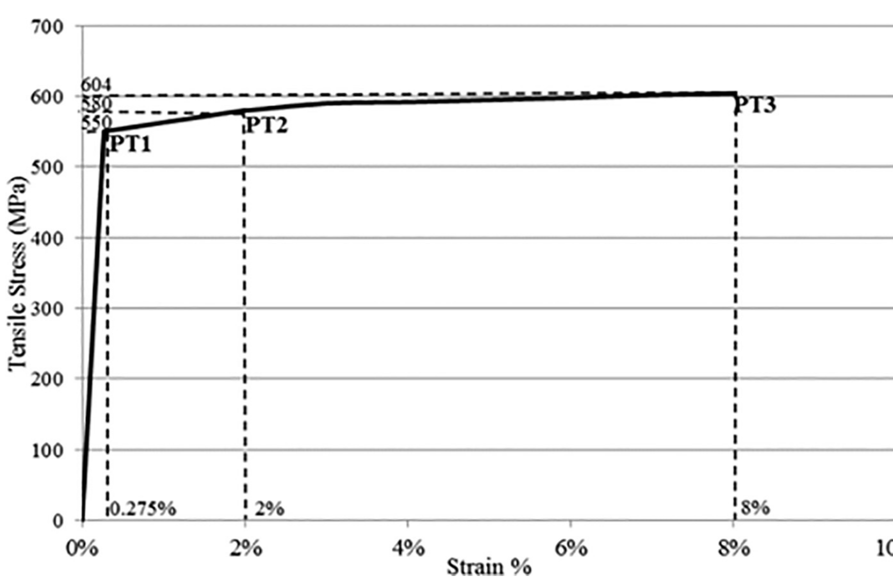

Fig. 4. Stress-strain curve for non-corroded steel bars.

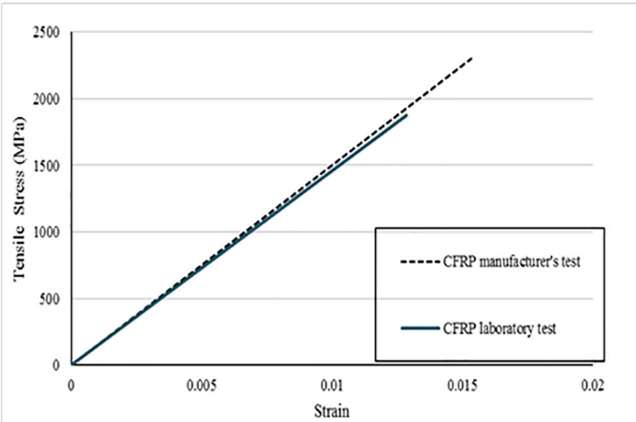

Fig. 5. Stress-strain curve for CFRP rods.

Table 4
Average values of steel bar properties.

Specimen Type	Young's modulus (GPa)	Yield Strength (MPa)	Ultimate Strength (MPa)	Ultimate strain
Corroded specimen	200	550	604	4%
Non-corroded specimen	200	550	645	8%

corroded bars were extracted from the beams, Table 4 shows the average steel bars properties.

Almahmoud et al. [43] tested the CFRP rods properties which are used in the present F.E model. The properties provided by the manufacturer and the laboratory are shown in Table 5.

4.2. Steel corrosion in the FE model

The corrosion of tensile steel bars is considered for all models of corroded beams studied in this paper (A1CL3-R, A2CL3 and A1CL3-RS). The corrosion of steel stirrups is neglected as it does not affect the flexural behavior. In addition, the steel cross-sectional area is reduced to the values which were obtained from the experimental studies. Table 6 shows the average cross-sectional area losses values which are considered in the FE models for all corroded beams.

Moreover, the stress-strain curve “post yielding behavior” is modified for the corroded steel bars. It was found experimentally by [19,33] that the corroded steel bars reach an ultimate strain value equivalent to half of that observed in the case of non-corroded steel bars, while no change was noticed regarding the yielding stress values. Fig. 6 shows the stress-strain curve for corroded steel bars which is implemented in the FE model.

Almassri et al. [23] proposed an innovative procedure to simulate the steel corrosion cracks using a special crack tool in ABAQUS. The same procedure is adopted here in order to construct a model for the corroded beams which have existing longitudinal cracks induced by steel corrosion. These preloading cracks are proposed to be in a symmetrical shape along the concrete cover and close to mid-beam (similar to the one found experimentally). Fig. 7 presents the steel corrosion cracks (in a red line).

Table 5
CFRP rod Properties.

Type of test	Ultimate strength (MPa)	Modulus of Elasticity (MPa)
Manufacturer's test	2300	150,000
Laboratory test	1875	145,900

5. Results and discussion

5.1. Moment deflection curves

The FE model predicts the global behavior of the 4 beams (A2CL3, A2T, A1T-R and A1CL3-R) which were studied experimentally. This can be observed from the moment-deflection curves presented in Fig. 8. The behavior of the new proposed model A1CL3-RS is also drawn along with the behavior of other beams in order to observe the change occurred in the behavior and the moment capacity due to the new proposed strengthening using the external steel plate.

The yielding moment capacity of the new model A1CL3-RS was recorded 65 KN.m and the ultimate moment capacity was 67 KN.m which is close to the ultimate capacity of A1T-R, a non-corroded beam repaired with NSM CFRP rod only. On the other hand, if it is compared to the beam A1CL3-R, a corroded beam which was repaired only with NSM, the yielding capacity of the later increased by 24 kN.m while the ultimate moment capacity increased by 16 kN.m.

5.2. Failure modes

One of the strengths of the FE model is that it can record the damages which happen in the reinforced concrete beams. The crack patterns are well predicted by the FE models. The main failure mode reported experimentally is concrete crushing which is either associated with a brittle failure in tensile steel bars due to corrosion or large flexural cracks in the tension zone. The FE model captures the cracks which occurred in the experiments for all common failure modes. (for beams A1T-R, A2T and A2CL3).

The following Figs. 9 and 10 show the FE crack patterns obtained in this study and the cracks patterns which were observed experimentally by previous studies, respectively.

Different from the common failure, the corroded beam A1CL3-R which was repaired using only NSM CFRP rod failed by separation of concrete cover as displayed in Fig. 10. The NSM technique was limited in repairing this corroded beam by this brittle premature failure.

The analytical and the FE model A1CL3-RS; which is a corroded beam repaired with both NSM CFRP rod and also with an external steel plate, failed due to large flexural cracks followed by concrete crushing as shown in Fig. 11. Therefore, using an external steel plate would change the failure mode and assist the NSM technique to reach to its maximum efficiency as discussed in the previous section.

5.3. Ductility and stiffness

The A1CL3-RS model is noticed to have less ductility index ($\varepsilon_u/\varepsilon_y$) than the corroded RC beam which was repaired using NSM only (A1CL3-R). A ductility index of 1.93 was calculated for A1CL3-RS while the experimental and FE ductility index values for A1CL3-R were found 7 and 4.5, respectively. On the other hand, the stiffness of the new model A1CL3-RS was found increased as it was observed in the linear stage. Fig. 12 shows the stiffness ratio (slope after repair / slope before repair) for the RC beams.

6. Analytical solution

The equations presented by Almahmoud et al. 2009 [21] are used here to calculate the yielding and ultimate moment capacity of NSM repaired RC sections. Eqs. (1) and (2) are listed below which calculate the yielding and ultimate moments. Fig. 13 shows strain and forces distribution for an RC section strengthened with an NSM CFRP rod.

$$M_n = nf_y fI_{yc}(d_s - y_0) \tag{1}$$

$$M_u = f_y fA_{ys}(d_s - 0.4y) + E_f A_f \varepsilon_c \frac{d_f - y}{y}(d_f - 0.4y) \tag{2}$$

Table 6
Average % of steel bars cross-sectional area losses due to corrosion.

Beam	Avg % of steel Area loss“beam's middle”	Description of Beam
A1Cl3-RS	20	Corroded Repaired with NSM and Steel Plate
A1Cl3-R	20	Corroded Repaired with NSM Only
A2CL3	21.5	Corroded Non-Repaired

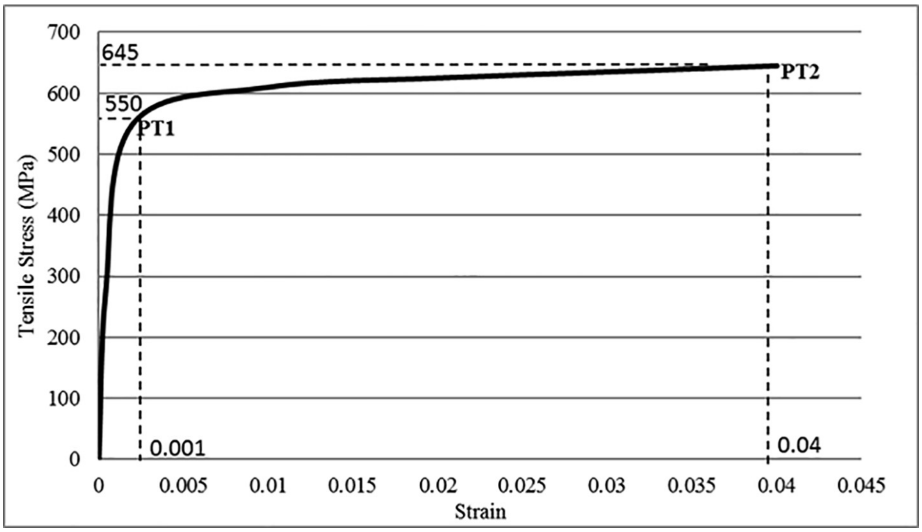

Fig. 6. Stress strain curve for corroded steel bars.

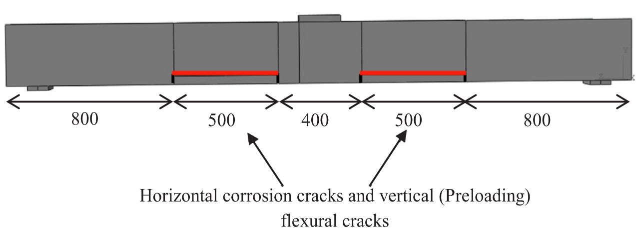

Fig. 7. Steel corrosion cracks implemented in the FE model.

Table 7 presents the calculated vs. the experimental values of yielding and ultimate moment capacity for all repaired beams.

As shown in Table 7, the premature mode of failure which occurred in beam A1CL3-R prevented the beam from reaching the maximum theoretical value of the classical failure mode. In this paper, one more beam is proposed (A1CL3-RS) which is repaired by using both a 6 mm rod of CFRP with NSM and using an external steel plate. This beam is a repaired beam with an NSM CFRP rod (having the same properties and geometry of A1CL3-R) and chemically bonded with an external steel plate as shown in Fig. 14.

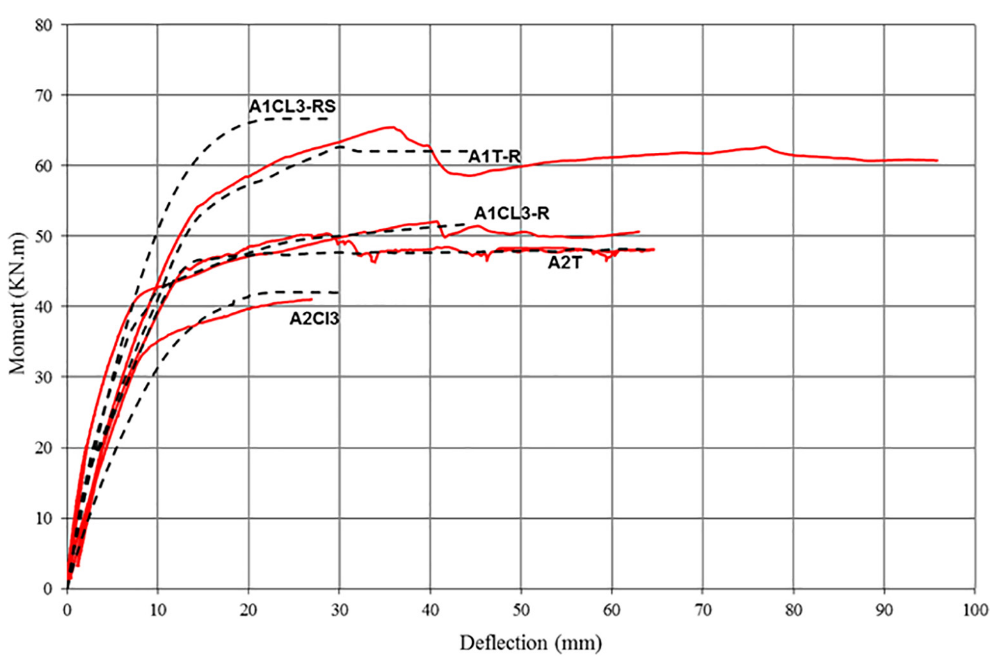

Fig. 8. Moment-deflection curves for all beams (Experimental and FE results).

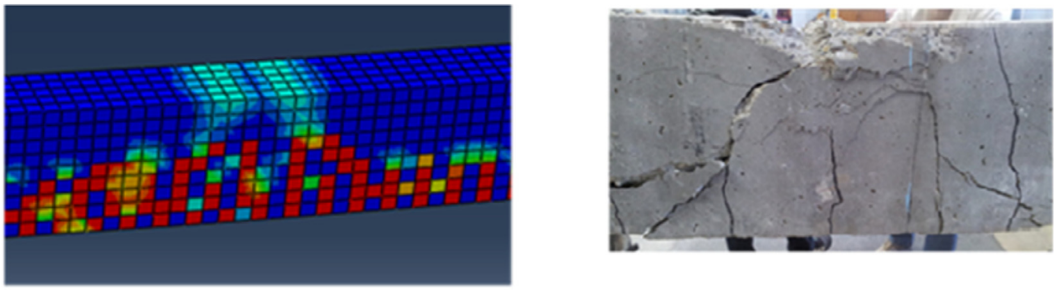

(a) F.E - A1T-R@A2T Control NSM repaired and N-Repaired (b) Exp. Classical mode of failure

Large flexural cracks followed by the concrete crushing

Fig. 9. Common mode of failure for the tested beams experimental and FE results.

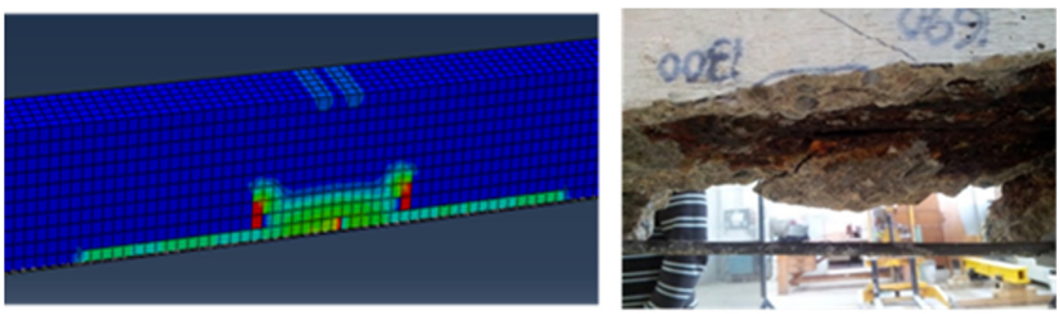

(a) F.E . A1CL3-R-Corroded repaired with NSM (b) Exp. Non classical mode of failure

separation of concrete cover without concrete crushing

or failure in tensile steel bar

Fig. 10. Non-Classical failure mode in the corroded repaired beam A1CL3-R.

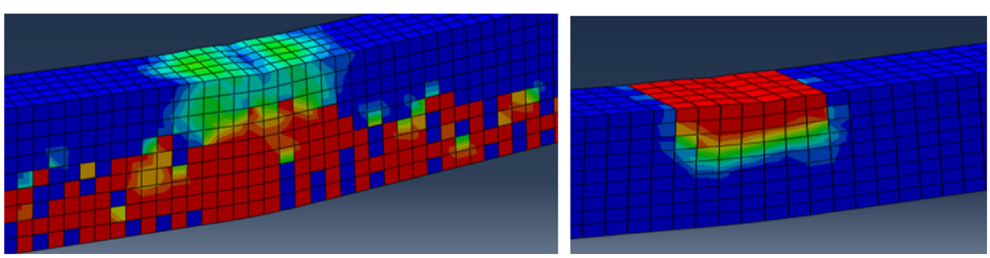

Fig. 11. FE mode of failure for the model A1CL3-RS.

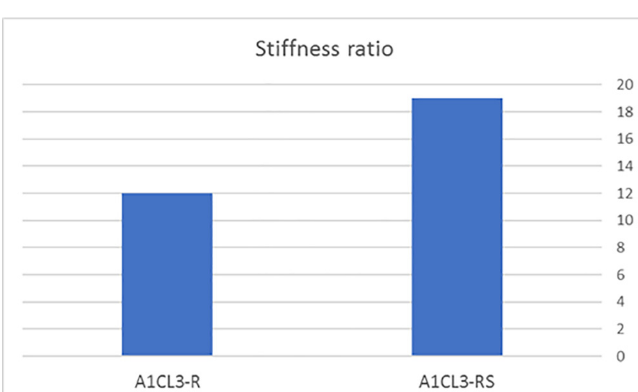

Fig. 12. Stiffness ratio.

Metwally [44] found that by increasing the steel plate thickness, the stiffness of the RC element increases. It was also found that any increase in plate thickness beyond 7 mm generates higher shear stresses on the contacting layer between concrete and steel plate, leading to debonding failure. In order to have a failure load less than the shear design capacity, a steel plate thickness of 1.5 mm and width of 120 mm are assumed for A1CL3-RS beam. ACI committee 318 [45] proposed an equation (*Eq. (1)*) which can predict the ultimate moment capacity of RC beams strengthened with epoxy steel plates:

$$M_n = A_{s1}f_{y1}\left(d_1 - \frac{\beta_1 c}{2}\right) + A_{sp}f_{yp}\left(d_p - \frac{\beta_1 c}{2}\right) \tag{3}$$

For beam A1CL3-RS, the predicted ultimate moment capacity can be calculated by using the equations presented in [21,39] simultaneously, (*as shown in Eq. (2)*):

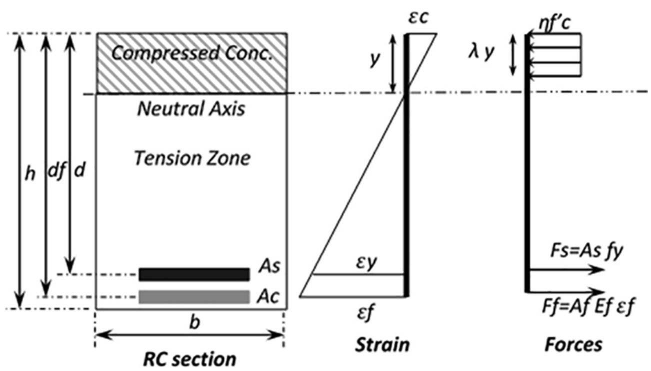

Fig. 13. Strain-Forces distribution for beams strengthened with NSM.

$$M_n = A_{s1} f_{y1} (d_s - 0.4y) + E_f .\ A_f .\ \varepsilon_{cu} . \left(\frac{d_f - y}{y}\right) . (d_f - 0.4y) + A_{sp} f_{yp} (d_p - 0.4y) \quad (4)$$

<u>*For A1CL3-RS:*</u> b = 15 cm, h = 28 cm, ds = 22.4 cm, Es = 200 GPa, Ef = 150 GPa, As = 3.42 cm^2, df = 27.3 cm Af = 0.28 cm^2, fy = 578 MPa, fyp = 420 MPa, Asp = (0.15 × 12) = 1.8 cm^2, dp = 28.1 cm. (Symbols denotations are listed in Appendix A.)

The ultimate moment capacity predicted for this beam (A1CL3-RS) is 76.5 KN.m as calculated from equation (2). On the other hand, the ultimate moment capacity found through the FE model is 67 KN.m, which is lower than expected analytically. The analytical model slightly overestimates the ultimate strength which is considered to be a predictable result.

7. Conclusions

The final conclusions of this study can be cast in the following remarks:

1. Defining preloading steel corrosion cracks in the FE model as well as using a special post-yielding behavior for the corroded steel bars show a satisfactory result in predicting the global behavior and the crack patterns of the corroded RC beams.
2. The NSM technique have some limitations in repairing naturally corroded RC beams. These limitations can be solved and the NSM technique can be enhanced by using an innovative hybrid strengthening solution which uses an external steel plate.
3. The three-dimensional FE model shows a good agreement with the experimental results in terms of the mechanical behavior as well as the failure modes.
4. The corroded RC beam repaired using NSM CFRP rod and an external steel plate shows an increase in terms of moment capacity and yielding capacity. It shows an ultimate moment capacity value close to a non-corroded "control" beam repaired with NSM only.
5. Using an external steel plate as an assistant repair technique for the corroded RC beams changes the failure mode form brittle to ductile one. It also slightly increases the stiffness and decreases the ductility.
6. This paper opens the door for future studies on using hybrid strengthening Techniques in the area of repairing corroded RC elements.

Declaration of Competing Interest

The authors declare that they have no known competing financial interests or personal relationships that could have appeared to influence the work reported in this paper.

Table 7
Calculated Vs Experimental yielding and ultimate moment values.

Beam	Description	Ultimate Moment (KN.m) Exp.	Ultimate Moment (KN.m) Calc.	Yielding Moment (KN.m) Exp.	Yielding Moment (KN.m) Calc.
A1Cl3-R	Corroded repaired with NSM Only beam	52	63.4	42	43.5
A1T-R	Control repaired beam with NSM only	66	68.4	53	51.7

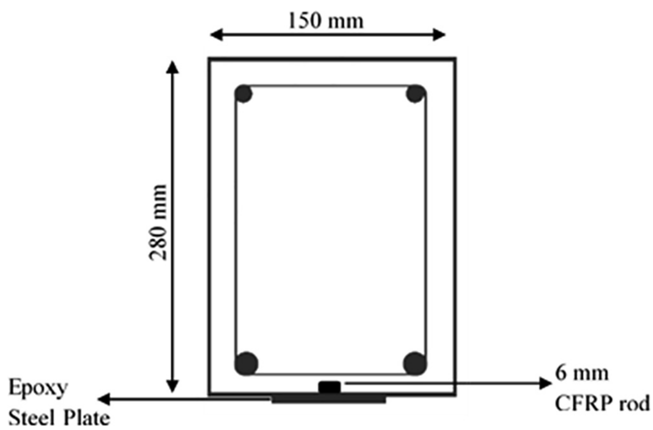

Fig. 14. A1CL3-RS proposed section.

Appendix A. (Symbols of the analytical model)

b = width of beam, h = depth of beam, ds = effective depth of steel bars, Es = young's modulus of steel, Ef = young's modulus of carbon, As = area of tensile steel bars, df = effective depth of CFRP, Af = area of CFRP rod, fy = yield stress of steel bars, fyp = yield stress of steel plate, Asp = area of steel plate, dp = effective depth of steel plateε_{cu} = ultimate strain in concrete, y = location of neutral axis N.A

References

[1] Rodriguez J, Ortega LM, Casal J. Load carrying capacity of concrete structures with corroded reinforcement. Constr Build Mater 1997 Jun 1;11(4):239–48.
[2] Huang R, Yang CC. Condition assessment of reinforced concrete beams relative to reinforcement corrosion. Cem Concr Compos 1997 Jan 1;19(2):131–7.
[3] Sæther I. Bond deterioration of corroded steel bars in concrete. Struct Infrastruct Eng 2011 Jun 1;7(6):415–29.
[4] Andrade C, Alonso C, Garcia D, Rodriguez J. Remaining lifetime of reinforced concrete structures: Effect of corrosion on the mechanical properties of the steel.
[5] Cairns J, Plizzari GA, Du Y, Law DW, Franzoni C. Mechanical properties of corrosion-damaged reinforcement. ACI Mater J 2005;102(4):256.
[6] François R, Khan I, Dang VH. Impact of corrosion on mechanical properties of steel embedded in 27-year-old corroded reinforced concrete beams. Mater Struct 2013;46(6):899–910.
[7] Su R, Zhu Y. Experimental and numerical studies of external steel plate strengthened reinforced concrete coupling beams. Eng Struct 2005;27(10):1537–50.
[8] Ziraba YN, Baluch MH. Computational model for reinforced concrete beams strengthened by epoxy bonded steel plates. Finite Elem Anal Des 1995 Sep 1;20(4):253–71.
[9] Zhang JW, Teng JG, Wong YL, Lu ZT. Behavior of two-way RC slabs externally bonded with steel plate. J Struct Eng 2001 Apr;127(4):390–7.
[10] Jumaat MZ, Alam MA. Plate bonded strengthened RC beams with end and intermediate anchors. Int J Eng Technol 2007;4(2):185–93.
[11] Arslan G, Sevuk F, Ekiz I. Steel plate contribution to load-carrying capacity of retrofitted RC beams. Constr Build Mater 2008;22(3):143–53.
[12] Sherwood EG, Soudki KA. Confinement of corrosion cracking in reinforced concrete beams using carbon fiber reinforced polymer laminates. Special Publication 1999;1(188):591–604.
[13] Soudki KA, Sherwood TG. Behaviour of reinforced concrete beams strengthened with carbon fibre reinforced polymer laminates subjected to corrosion damage. Can J Civ Eng 2000 Oct 1;27(5):1005–10.
[14] Steiner W. Strengthening of structures with CFRP strips. InAdvanced Composite Materials in Bridges and Structures 1996 Aug 11 (pp. 407-419). Canadian Society for Civil Engineers, Montreal, Quebec, Canada.
[15] Bilotta A, Ceroni F, Di Ludovico M, Nigro E, Pecce M, Manfredi G. Bond efficiency of EBR and NSM FRP systems for strengthening concrete members. J Compos Constr 2011;15(5):757–72.
[16] De Lorenzis L, Teng JG. Near-surface mounted FRP reinforcement: An emerging technique for strengthening structures. Compos B Eng 2007;38(2):119–43.
[17] Al-Mahmoud F, Castel A, François R, Tourneur C. RC beams strengthened with NSM CFRP rods and modeling of peeling-off failure. Compos Struct 2010;92(8):1920–30.
[18] Kreit A, Al-Mahmoud F, Castel A, François R. Repairing corroded RC beam with near-surface mounted CFRP rods. Mater Struct 2011;44(7):1205–17.
[19] Almassri B, Kreit A, Al Mahmoud F, François R. Mechanical behaviour of corroded RC beams strengthened by NSM CFRP rods. Compos B Eng 2014;1(64):97–107.
[20] Hawileh RA. Nonlinear finite element modeling of RC beams strengthened with NSM FRP rods. Constr Build Mater 2012;27(1):461–71.
[21] Al-Mahmoud F, Castel A, François R, Tourneur C. Strengthening of RC members with near-surface mounted CFRP rods. Compos Struct 2009;91(2):138–47.
[22] Barros JA, Baghi H, Dias SJ, Ventura-Gouveia A. A FEM-based model to predict the behaviour of RC beams shear strengthened according to the NSM technique. Eng Struct 2013;1(56):1192–206.
[23] Almassri B, Al Mahmoud F, Francois R. Behaviour of corroded reinforced concrete beams repaired with NSM CFRP rods, experimental and finite element study. Compos B Eng 2016;1(92):477–88.
[24] Al-Osta MA, Al-Sakkaf HA, Sharif AM, Ahmad S, Baluch MH. Finite element modeling of corroded RC beams using cohesive surface bonding approach. Computers Concr 2018;22(2):167–82.
[25] Zhang S. Behaviour and modelling of RC beams strengthened in flexure with near-surface mounted FRP strips.
[26] Soliman SM, El-Salakawy E, Benmokrane B. Bond performance of near-surface-mounted FRP bars. J Compos Constr 2011;15(1):103–11.
[27] Kreit A, Al-Mahmoud F, Castel A, Francois R. Corroded RC beam repaired with near-surface mounted CFRP rods. InInternational conference on concrete repair, rehabilitation and retrofitting, Cape Town, South Africa 2008 Nov (pp. 24-26).
[28] Rezazadeh M, Barros JA, Ramezansefat H. End concrete cover separation in RC structures strengthened in flexure with NSM FRP: Analytical design approach. Eng Struct 2016;1(128):415–27.
[29] Teng JG, Zhang SS, Chen JF. Strength model for end cover separation failure in RC beams strengthened with near-surface mounted (NSM) FRP strips. Eng Struct 2016;1(110):222–32.
[30] ABAQUS version 6.14.1 (2014). [Computer software]. Assault Systems. Waltham. MA.
[31] Castel A, François R, Arliguie G. Mechanical behaviour of corroded reinforced concrete beams—Part 1: Experimental study of corroded beams. Mater Struct 2000;33(9):539–44.
[32] Vidal T, Castel A, Francois R. Corrosion process and structural performance of a 17 year old reinforced concrete beam stored in chloride environment. Cem Concr Res 2007;37(11):1551–61.
[33] Dang VH, Francois R. Influence of long-term corrosion in chloride environment on mechanical behaviour of RC beam. Eng Struct 2013;1(48):558–68.
[34] Khan I, François R, Castel A. Structural performance of a 26-year-old corroded reinforced concrete beam. Eur J Environ Civil Eng 2012;16(3–4):440–9.
[35] Sena Cruz JM, Barros JA, Gettu R, Azevedo AF. Bond behavior of near-surface mounted CFRP laminate strips under monotonic and cyclic loading. J Compos Constr 2006;10(4):295–303.
[36] Abaqus I. Abaqus user's manual. Dassault Systemes, Rhode Island, USA: ABAQUS Inc; 2007.
[37] Tahnat YB, Dwaikat MM, Samaaneh MA. Effect of using CFRP wraps on the strength and ductility behaviors of exterior reinforced concrete joint. Compos Struct 2018;1(201):721–39.
[38] Tahnat YB, Samaaneh MA, Dwaikat MM, Halahla AM. Simple equations for predicting the rotational ductility of fiber-reinforced-polymer strengthened reinforced concrete joints. Structures. Elsevier; 2020. p. 73–86.
[39] Halahla AM, Tahnat YB, Almasri AH, Voyiadjis GZ. The effect of shape memory alloys on the ductility of exterior reinforced concrete beam-column joints using the damage plasticity model. Eng Struct 2019;1(200):109676.
[40] Ho NM, Lima MM, Doh JH. Axially loaded three-side restrained reinforced concrete walls: a comparative study. InMechanics of Structures and Materials XXIV: Proceedings of the 24th Australian Conference on the Mechanics of Structures and Materials (ACMSM24, Perth, Australia, 6-9 December 2016) 2016 Nov 30 (p. 65). CRC Press.
[41] Alhassan MA, Al-Rousan RZ, Hejazi MA. Novel Nonlinear Model for Analysis of RC Slabs with Various Boundary Conditions Under Monotonic Loading. Int Rev Civil Eng (IRECE) 2018;9(6):218.
[42] Wahalathantri BL, Thambiratnam DP, Chan TH, et al. A material model for flexural crack simulation in reinforced concrete elements using ABAQUS. In: First international conference on engineering, designing and developing the built environment for sustainable wellbeing, Brisbane, Australia, 28 Apr 2011, pp. 260-264. Queensland University of Technology.
[43] Almahmoud F, Castel A, François R, Tourneur C. Effect of surface pre-conditioning on bond of carbon fibre reinforced polymer rods to concrete. Cem Concr Compos 2007 Oct 1;29(9):677–89.
[44] Metwally IM. Three-dimensional finite element analysis of reinforced concrete slabs strengthened with epoxy-bonded steel plates. Adv Concr Constr 2014 Jun 1;2(2):091.
[45] Standard AA. Building Code Requirements for Structural Concrete (ACI 318-11). 2011.